THE JOURNAL OF PHYSICAL CHEMISTRY B

Article

pubs.acs.org/JPCB

Study of Complex Thermosensitive Amphiphilic Polyoxazolines and Their Interaction with Ionic Surfactants. Are Hydrophobic, Thermosensitive, and Hydrophilic Moieties Equally Important?

Anna Bogomolova,[†] Sergey K. Filippov,*[,†] Larysa Starovoytova,[†] Borislav Angelov,[†] Petr Konarev,[‡] Ondrej Sedlacek,[†] Martin Hruby,[†] and Petr Stepanek[†]

[†]Institute of Macromolecular Chemistry AS CR, v.v.i, Heyrovsky Sq. 2, 162 06 Prague 6, Czech Republic

[‡]European Molecular Biology Laboratory, EMBL c/o DESY, Notkestrasse 85, Hamburg D-22603, Germany

Supporting Information

ABSTRACT: The temperature-driven self-assembly of nonionic amphiphilic tailor-made triblock copolymers has been studied by DLS, NMR, ITC, and SAXS. The composition of these triblock copolymers is more complex than that of the vast majority of poly(2-alkyl-2-oxazoline)s: a statistical thermoresponsive (iPrOx) and hydrophobic (BuOx) central block with terminal hydrophilic blocks (MeOx). In general, as temperature increases, nanoparticles form in a process starting with single molecules that become loose aggregates and ends with the formation of compact nanoparticles. Here, we first attempt to resolve the effects of each block on nanoparticle formation. It has been proven that the iPrOx/MeOx ratio determines the value of the cloud point temperature, whereas the different BuOx−iPrOx blocks determine the character of the process. Finally, we complete our investigation by presenting the thermodynamic and structural profiles of the complexation between these triblock poly(2-alkyl-2-oxazoline)s and two ionic surfactants. The addition of an ionic surfactant promotes a rearrangement of the polymer molecules and the formation of complexes followed by the appearance of polymer−surfactant hybrid micelles. Analysis of the interaction shows a strong and nonspecific reaction between the polymers and the anionic surfactant sodium dodecyl sulfate and weak but polymer-state-sensitive interactions between the polymer and the cationic surfactant hexadecyltrimethylammonium bromide.

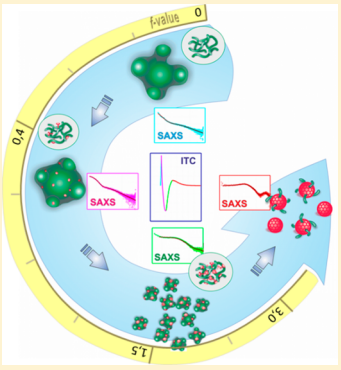

INTRODUCTION

Poly(2-alkyl-2-oxazoline)s are polymers that are currently widely and intensively investigated for biomedical purposes. Numerous articles have been devoted to the properties and applications of poly(2-alkyl-2-oxazoline)s in different fields, including drug delivery, tumor diagnostics, and antimicrobial agents.[1−4] The properties of these polymers depend on the alkyl group. The presence of a methyl or ethyl substituent (MeOx) makes the polymer hydrophilic, whereas poly(2-isopropyl-2-oxazoline) (iPrOx) shows thermoresponsive properties, and poly(2-butyl-2-oxazoline) (BuOx) and poly(2-phenyl-2-oxazoline) have hydrophobic natures.[2]

The synthesis of complex polymers from blocks with different structures makes it possible for the system to form specific structures.[5,6] It was previously shown that triblock copolymers constructed from a central block (statistical copolymer of BuOx and iPrOx) with terminal MeOx blocks can form a micelle-like structure as the temperature increases.[7] The onset of the transition from a molecular state to a micelle-like state has been defined as the cloud point temperature (CPT), and CPT has been shown to strongly depend on the ratio of thermoresponsive to hydrophilic blocks. Moreover, the introduction of a phenolic moiety into the copolymer allowed radionuclide labeling with iodine-125 for a promising use of the system in tumor diagnostics.

The structure of these copolymers appears to be very similar to the structure of Pluronic molecules, the triblock copolymers PEO−PPO−PEO, with their amphiphilic nature and the ability to self-assemble at a certain temperature.[8,9] Pluronic molecules have found wide application in biomedicine and are commonly used in a combination with normal ionic surfactants.[10] Recently, several experiments were performed using Pluronic systems in combination with ionic surfactants. It was shown that the ionic surfactants bind strongly with the polymer molecules and subsequently decrease the aggregation number of the block copolymer.[11−15]

Here, we investigate the behavior of the nonionic amphiphilic triblock copolymers MeOx-stat-(iPrOx-*co*-BuOx)-MeOx as the temperature increases. The backbone, which is constructed from poly(2-alkyl-2-oxazoline) units, makes this copolymer very attractive for biomedical applications. Its complex structure and similarity to Pluronic-like molecules allow for its use as an active species for tumor diagnostics. However, the units in the central block of this copolymer are arranged in a statistical manner, in contrast to the Pluronic molecules, making this system more complex. How does each

Received: January 31, 2014
Revised: April 15, 2014
Published: April 18, 2014

Scheme 1. Chemical Structure and Schematic Image of the Polymer under Investigation

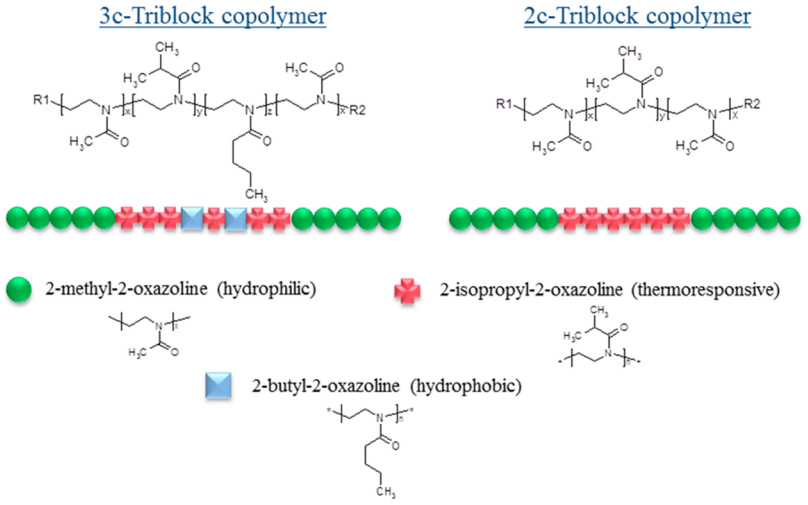

Table 1. Molecular Characteristics of the Polymers (c = 1.4 wt %)[a]

				n_{MeOx}		n_{iPrOX}		n_{BuOX}	
				NMR	NMR	NMR	NMR	NMR	NMR
polymers	type of polymer	2-butyl-2-oxazoline in thermoresponsive block, mol %	CPT, °C	H_2O	$CDCl_3$	H_2O	$CDCl_3$	H_2O	$CDCl_3$
MeOx	homopolymer	0	N/A		72				
IrOx	homopolymer	0	57				67		
oxBlock	2c-triblock copolymer	0	44	84	84	23	25.5		
ox(2:1)	3c-triblock copolymer	15	19	31.5	31.5	39	52.5	10	10.5
ox(1:1)	3c-triblock copolymer	15	17		52		40		8
ox(1:2)	3c-triblock copolymer	15	24	72	72	21	27	4.5	6

[a]The NMR data were obtained at 17 °C.

block in the molecule affect nanoparticle formation? To determine the answer to this question, we performed dynamic light scattering (DLS), small-angle X-ray scattering (SAXS), and nuclear magnetic resonance (NMR) experiments on three copolymers with different ratios of thermoresponsive to hydrophilic groups. Bearing in mind that a great attention was given for the characterization of Pluronic molecules in systems with ionic surfactants, we also analyzed the binding isotherm of copolymers with the anionic surfactant sodium dodecyl sulfate (SDS) and the cationic surfactant hexadecyltrimethylammonium bromide (CTAB) by isothermal titration calorimetry (ITC). Such knowledge will be extremely useful for understanding the nature of the interaction between amphiphilic poly(2-alkyl-2-oxazoline) molecules with the surfactant-like amphiphilic drugs that are used in micellar drug delivery systems; these drugs include the antibiotics doxorubicin (antineoplastic agent), monensin (a coccidiostat), amphotericin B, and nystatin (polyene antimycotic). To the best our knowledge, this study is the first in which the role of hydrophobic/hydrophilic/thermosensitive blocks and their interactions with surfactants were analyzed using polyoxazolines.

MATERIALS AND METHODS

Materials. Triblock copolymers were synthesized according to the scheme published in a previous article.[7] The chemical structure and composition of the polymers (three component (3c) and two component (2c) triblock copolymers) are indicated in Scheme 1 and Table 1. The 2c triblock was synthesized for comparative purposes; the 2c triblock copolymer possesses no hydrophobic BuOx groups. The molecular weights of polymers were ca. 10 kDa (roughly 100 monomeric units), and the polydispersities of the samples according to ref 7 were 1.39. Water was deionized with a Millipore Milli-Q water purification system. Sodium dodecyl sulfate and cetyltrimethylammonium bromide were purchased from Sigma-Aldrich Ltd. (Prague, Czech Republic). SDS was recrystallized from hexane, and the other chemicals were used without additional purification.

Methods. *Dynamic Light Scattering.* The temperature-induced micelle formation in aqueous solutions, the temperature dependences of the apparent hydrodynamic radius of particles, R_h, and the scattering intensity, I_s, were automatically measured at a scattering angle of $\theta = 173°$ on a Zetasizer Nano-ZS instrument, Model ZEN3600 (Malvern Instruments, UK). The DTS (Nano) program was used to evaluate the data. It provides an intensity-, volume-, and number-weighted R_h distribution function $G(R_h)$. A volume-weighted value of the apparent R_h was chosen to monitor the temperature changes in the system because it provides a realistic measure of the characteristic particle size in a solution. The temperature dependence of the nanoparticle formation was measured by heating from 5 to 55 °C in steps of 1 °C. Three measurements were taken after a steady-state condition was reached after each temperature change.

If not otherwise stated, all measurements were conducted with a polymer concentration of 1.4 mM (14 mg/mL) in water, and all solutions were filtered through a 0.22 mm PVDF syringe filter before measurement. The molecular characteristics of the polymers are presented in Table 1.

dx.doi.org/10.1021/jp5011296 | J. Phys. Chem. B 2014, 118, 4940−4950

Nuclear Magnetic Resonance (NMR). To characterize the behavior of the polymer system, the ^{1}H and ^{1}H spin−spin relaxation times T_2 were measured using NMR spectroscopy at different temperatures. Relaxation NMR spectroscopy is a useful tool for investigating polymer and solvent dynamics due to the fact that the transverse magnetization component is sensitive to changes in the mobility of polymer segments as well as the solvent.

^{1}H NMR measurements were performed with a Bruker Avance III 600 spectrometer operating at 600.13 MHz. The integrated intensities were determined with the spectrometer integration software at an accuracy of ±1%. In all measurements, the temperature was maintained at a constant value within ±0.2 K using a BVT 3000 temperature unit. The typical measurement conditions were as follows: 90 pulses with a width of 10 μs, relaxation delay of 10 s, spectral width of 5995.204 Hz, and 32 scans in the temperature range 17−57 °C. The ^{1}H spin−spin relaxation times T_2 for all components were measured using the CPMG pulse sequence $90°_x$-(t_d-$180°_y$-t_d)n-acquisition with t_d = 0.5 ms. Each experiment was conducted with 16 scans, a relaxation delay of 100 s, and a spectral width of 10 kHz.

Two types of deuterated solvents were used for the experiments. Chloroform, in which all of the polymer blocks are fully soluble, was used as the solvent for the structure analysis of each block in the copolymers. In aqueous solution, the intensity of the iPrOx and BuOx blocks is affected by the thermoresponsive behavior of the copolymer. The molecular parameters obtained for the polymers in water and in chloroform at 17 °C are presented in Table 1.

Isothermal Titration Calorimetry. The microcalorimetry study was performed using a MicroCal 200 isothermal titration calorimeter. The experiment was performed with consecutive injections of the concentrated surfactant solution into the calorimeter cell; the cell contained 280 μL of the polymer or water solution (14 mg/mL). A surfactant solution was added from a 40 μL injection syringe, the tip of which was modified to act as a stirrer. The chosen stirring speed was 1000 rpm. The injection volume varied between 1 and 2 μL. The time between injections was usually 5 min. The measurements were conducted at 15, 25, and 41 °C. The data were analyzed using Microcal ORIGIN software. The experimental enthalpy was obtained by integrating the raw data signal. The integrated molar enthalpy change per injection was obtained by dividing the experimentally measured enthalpy by the number of moles of surfactant added. The final enthalpograms are the plots of the integrated molar enthalpy as a function of total surfactant concentration in the calorimeter sample cell.

Small-Angle X-ray Scattering. Synchrotron SAXS experiments were performed at EMBL beamline P12 (Petra III, Hamburg, Germany) using a pixel detector (2 M PILATUS). The X-ray scattering images were recorded at a sample−detector distance 2.7 m, using a monochromatic incident X-ray beam (λ = 0.125 nm) covering the range of momentum transfer of 0.05 nm^{-1} < q < 3.5 nm^{-1} ($q = 4\pi \sin\theta/\lambda$, where 2θ is the scattering angle). No measurable radiation damage was detected in most of the samples, as determined by comparing 20 successive time frames that had 50 ms exposure times. In all cases reported in this paper, the two-dimensional scattering patterns were isotropic. The patterns were azimuthally averaged to determine the dependence of the scattered intensity $I_s(q)$ on the momentum transfer q. The solvent scattering was subtracted prior to the fitting analysis.

All data manipulations were performed using PRIMUS software.[16,17]

Another set of SAXS experiments was performed on the high brilliance beamline ID02 at ESRF (Grenoble, France). The SAXS setup utilizes a pinhole camera with a beam stop placed in front of a two-dimensional Frelon CCD detector. The X-ray scattering patterns were recorded for sample-to-detector distances of 1.5 and 8 m, using a monochromatic incident X-ray beam with an energy E = 12 460 eV (λ = 0.1 nm). The available wave vector range was q = 0.05−2.76 nm^{-1}. Online corrections were applied for the detector, and the sample/detector distance, center, transmission, and incident intensity were calibrated. All the cases reported in this paper have isotropic scattering; thus, azimuthal regrouping and radial averaging were also performed online to determine the dependence of the scattered intensity $I_s(q)$ on the scattering vector q in absolute units. The scattering from a capillary filled with Milli-Q water was measured for use as a background and subtracted from the scattering signals of the samples. Prior to the experiment, a representative sample was checked for radiation damage.

RESULTS AND DISCUSSION

DLS analysis of the systems of triblock copolymers was performed at a polymer concentration of 1.4 mM, which was considered appropriate for the subsequent ITC experiments. The previous DLS results for 3c-triblock copolymers (concentration 0.05 mM)[7] indicate the presence of single molecules of a polymer (radius ca. 2−3 nm) at temperatures below CPT and the formation of large aggregates as the temperature increased above CPT (radius ca. 100−300 nm) (Figure 1). However, in addition to the previous results, we observed a consecutive transformation of the aggregates into compact nanoparticles (ca. 25 nm) at the highest temperature, 50 °C. (Figure 1). One can suggest that the loose aggregates that initially formed at CPT shrank above CPT in the surrounding conditions as a result of the thermosensitivity of the polymers.

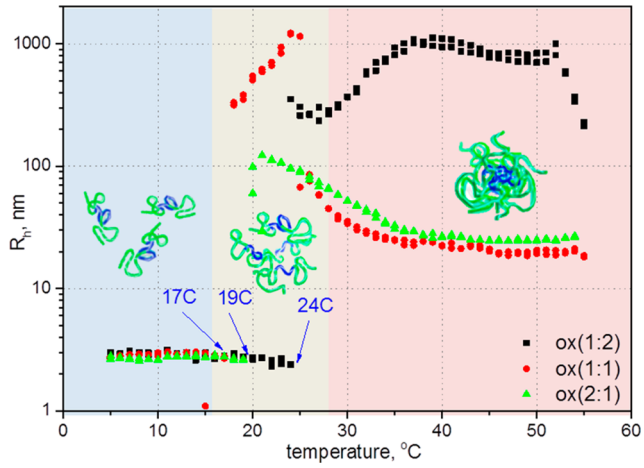

Figure 1. DLS data from pure 3c-triblock poly(2-alkyl-2-oxazoline)s, C = 14 mg/mL.

Comparing the DLS data from polymers with different ratios of hydrophobic/hydrophilic groups allows for an assessment of the influence of this ratio on the process of complex formation. The hydrophobic group content was slightly varied for all three

dx.doi.org/10.1021/jp5011296 | J. Phys. Chem. B 2014, 118, 4940−4950

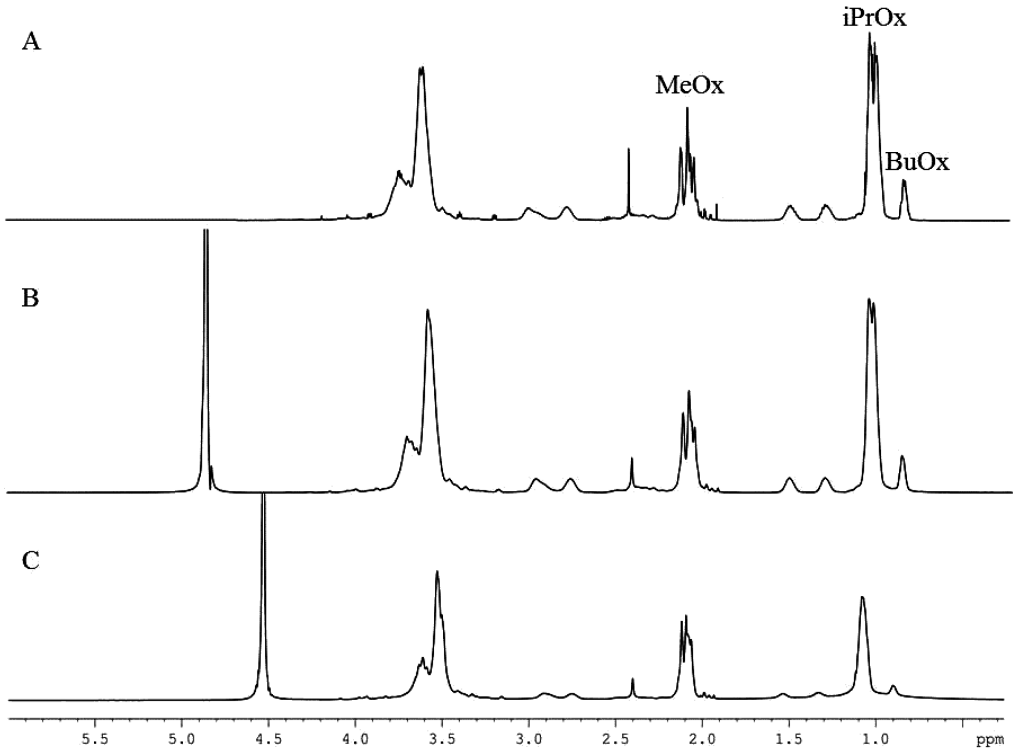

Figure 2. ^{1}H spectra of ox(2:1) copolymers (A) in $CDCl_3$ at 17 °C, (B) D_2O at 17 °C, and (C) D_2O at 57 °C.

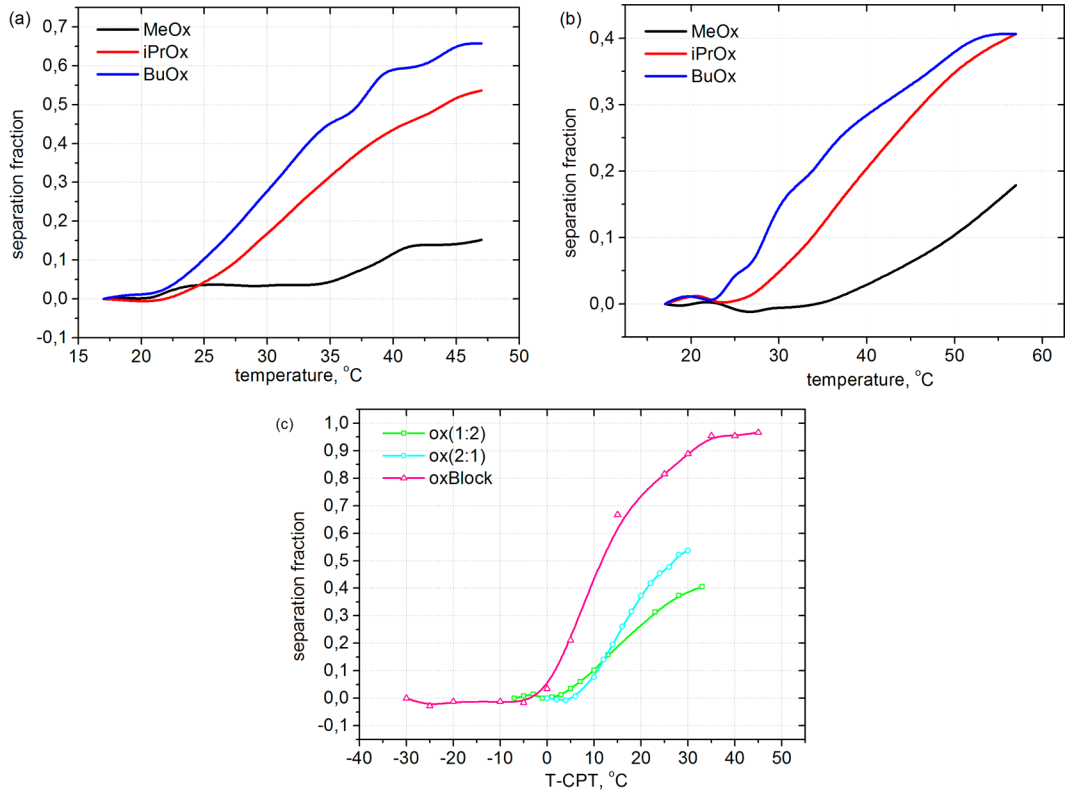

Figure 3. NMR data for the separation parameter as a function of temperature for (a) ox(2:1), (b) ox(1:2), and (c) iPrOx for ox(2:1), ox(1:2), and oxBlock.

investigated 3c-triblock copolymers (Table 1). There is only one significant difference in the experimental set—the ratio of units in the central and terminal blocks. An excess of hydrophobic and thermoresponsive groups leads to a decrease in CPT to 19 °C and to the formation of a rather compact structure right above the transition temperature. At the same time, increasing the number of hydrophilic groups contributes to the shift of the CPT to a higher value. The complex

dx.doi.org/10.1021/jp5011296 | J. Phys. Chem. B 2014, 118, 4940−4950

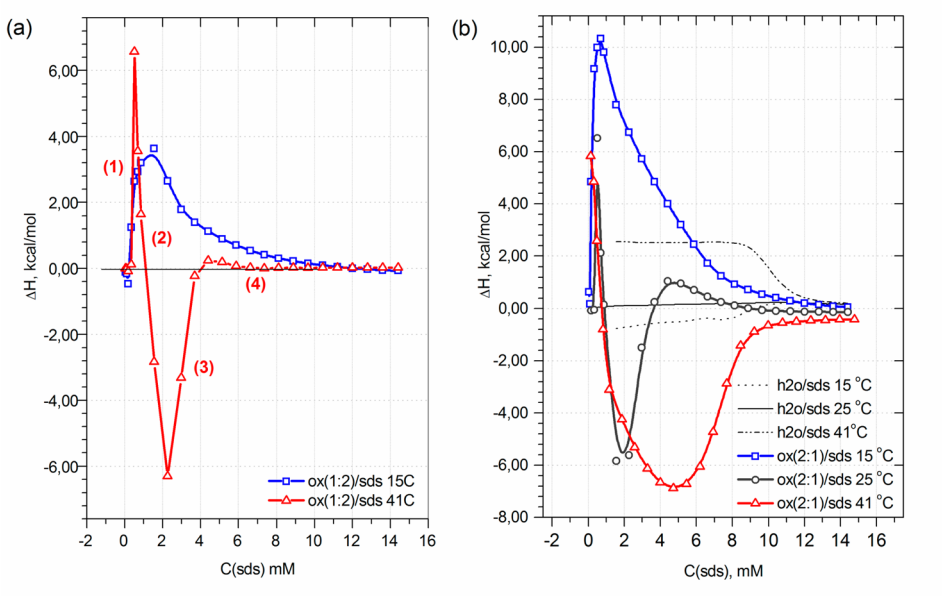

Figure 4. ITC curve for SDS titration of polymers at different temperatures: (a) ox(2:1) and (b) ox(1:2).

Table 2. Parameters of the Interaction between the Polymers and Surfactant

surfactant	cmc,[a] mM	cac[b] (molecular state), mM	cac (micellar state), mM	C_2, mM
SDS	8.4	0.15	0.35	12−14
CTAB	1.25	0.7	0.07	>20

[a]The cmc is taken from the blank titration of surfactant to water and does not show a significant variation with temperature. [b]The cac is an average value across all polymers; the molecular state and the micellar state correspond to the conformation of the polymer at 15 and 25 (or 41) °C, respectively.

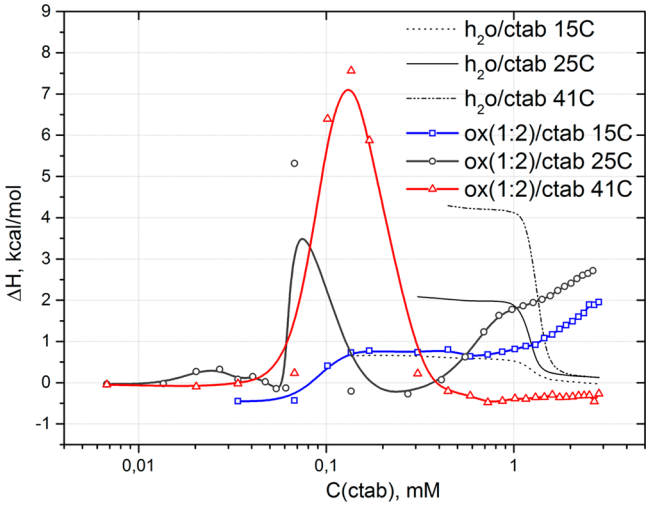

Figure 5. ITC curve for the titration of the polymer ox(1:2) with CTAB at different temperatures.

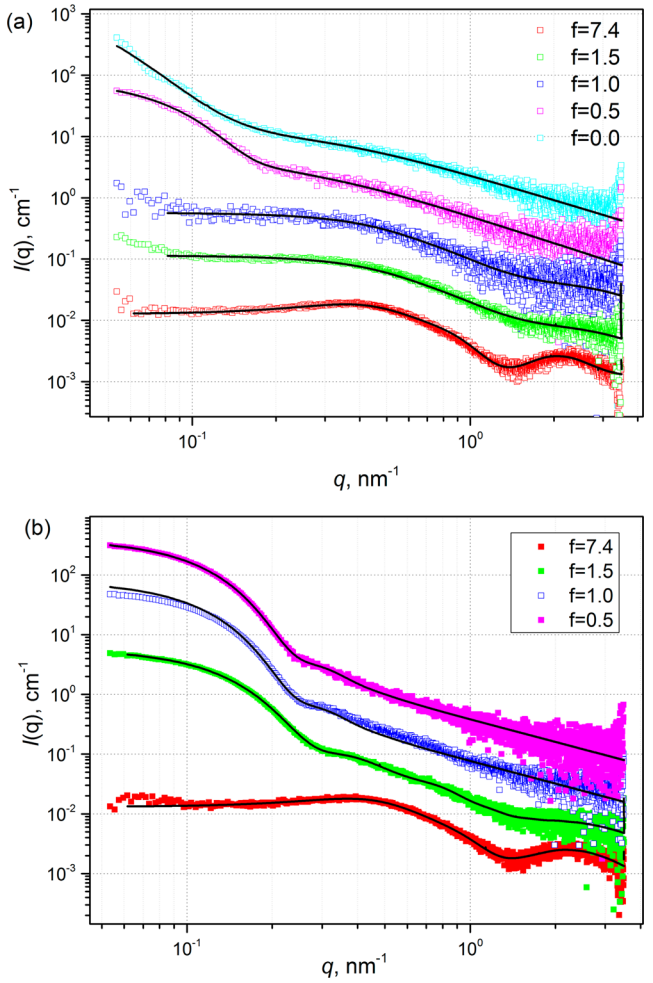

Figure 6. SAXS curves for solutions of the ox(1−1) copolymer and SDS taken at T = 25 °C (a) and T = 40 °C (b). The solid lines are fits. Each curve is shifted by a factor of 5 from top to bottom for clarity.

formation that is observed using DLS as the temperature increases can be described as a two-step process (red curve in Figure 1). In the first step, one can observe large aggregates with a hydrodynamic radius of up to 103 nm; with further temperature increases, the aggregates transformed into particles with a radius ca. 25−30 nm. For the ox(1:2) copolymer with the largest amount of hydrophilic MeOx groups, we detected an extended transition into compact structures (Figure 1). The

dx.doi.org/10.1021/jp5011296 | J. Phys. Chem. B 2014, 118, 4940−4950

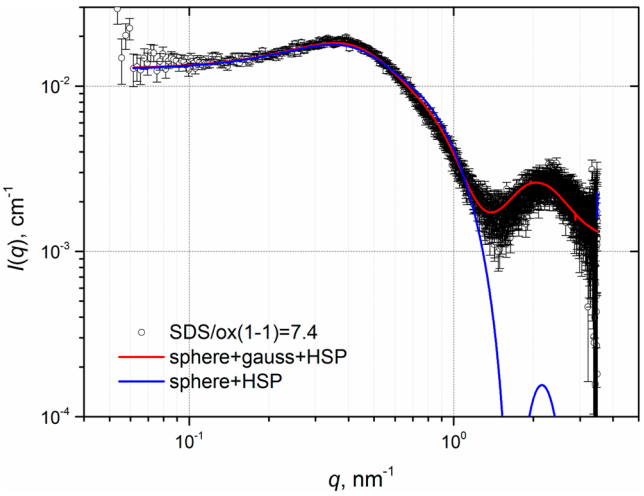

Figure 7. SAXS curve for solutions of ox(1:1) copolymer and SDS taken at T = 25 °C; f = 7.4.

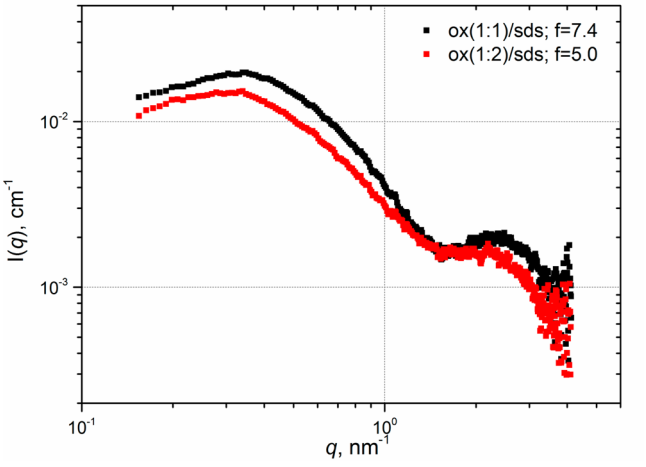

Figure 8. SAXS curves for solutions of ox(1:1) and of ox(1:2) polymers and SDS taken at T = 25 °C.

temperature dependence obtained for the 2c-triblock copolymer that was constructed from only the central thermoresponsive group with hydrophilic terminal groups exhibits similar behavior (Figure 1S, Supporting Information). One can conclude that addition of hydrophobic groups to the central block (at the same ratio of thermoresponsive/hydrophilic groups) causes the shift in the CPT value but does not influence the process of particle formation. Thus, we can consider the ox(1:2) sample to be a more hydrophilic polymer, whereas the ox(2:1) polymer demonstrates more hydrophobic properties.

NMR analysis was conducted for the pure polymers in the same conditions as mentioned above. The separation fraction was chosen to assess the mobility of the different groups as the temperature varied. The thermosensitivity of some polymer blocks restricted the mobility of polymer segments, thus causing the spectrum of a copolymer in water (Figure 2B,C) to differ from that in chloroform (Figure 2A). This restriction results in broadening and a significant decrease in the integrated intensity of the corresponding NMR signals. For comparative analysis, the values of the separation fraction p were calculated as

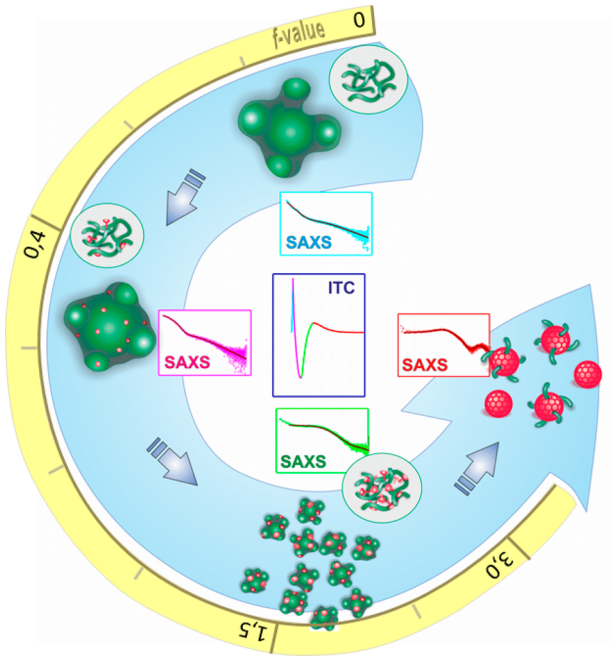

Figure 9. Structure sequence of the complexation process of triblock poly(2-alkyl-2-oxazolines) with increasing the concentration of surfactants.

$$p = 1 - I_T/I_0$$

where I_T is the integrated intensity of the polymer peak in a partly separated system and I_0 is the initial value of integrated intensity of the corresponding peak. The separation fraction p can be determined for all polymer segments separately.[18−22]

Preliminary analysis of the experimental data (Figure 3a,b) shows that the separation fraction, which corresponds to BuOx and iPrOx groups, sharply changes with temperature and reaches a value of 0.5−0.7 for the ox(2:1) copolymer (47 °C) and 0.4 for ox(1:2) (57 °C). We did not detect any significant differences in the temperature (21−23 °C) at which the group mobility began to decrease for the two polymers. This situation becomes clear if we account the fact that the NMR measurement was conducted in water and that the signal intensity of groups at 17 °C was taken as an initial parameter. Comparing the results obtained at 17 °C in water and in d-chloroform shows a very interesting fact: while the CPT for ox(2:1) was approximately 17 °C, the mobility of the iPrOx group at this temperature had already been reduced by a factor of 25%; this decrease was 22% for copolymer ox(1:2) at 24 °C (Table 1). At the same time, we did not observe any significant changes between the mobilities of the BuOx groups at 17 °C in water and in d-chloroform. Previous analysis and the fact that the separation fraction for the BuOx and iPrOx groups shows synchronous changes with increasing temperature support the initial suggestion about the statistical order of the units in the central block of copolymers. Thus, we can consider the central block to be a single entity and the whole copolymer to be similar to a Pluronic molecule with central thermoresponsive/hydrophobic blocks and terminal hydrophilic blocks. Moreover, we also observed some changes in the mobility of the MeOx group with increasing temperature. These changes most likely result from the aggregation of the central block that reduces the mobility of the nearby MeOx units and, as a result, slightly increases the separation fraction. Comparing the separation

dx.doi.org/10.1021/jp5011296 | J. Phys. Chem. B 2014, 118, 4940−4950

Table 3. Fitting Parameters for ox(1-1) and SDS at T = 25 and 40 °C

		form factor								
		big spherical particles, q > 0.2 nm^{-1}		generalized Gaussian coil		sphere with attaches Gaussian coil			structure factor	
f	T, C	R_{big}, Å ± 1	sigma ±0.01	R_g, Å	ν	R, Å	R_g, Å	sigma	RHS, Å ± 0.1	f_b, 10^{-2}
0	25	>200	0.86	37.3 ± 0.2	0.72 ± 0.02					
0.5	25	200	0.25	42.3 ± 0.3	0.66 ± 0.02					
0.5	40	167	0.19	37.5 ± 0.5	0.77 ± 0.04					
1.0	25					23 ± 4	4.8 ± 0.8	0.7 ± 0.2	63.9	2 ± 1
				33.7 ± 0.5	0.53 ± 0.03					
1.0	40	163	0.17			22 ± 2	1 ± 4	0.44 ± 0.08	93.2	8 ± 6
		163	0.15	56.2 ± 0.6	0.73 ± 0.02					
1.5	25					18.9 ± 0.4	5.4 ± 0.2	0.70 ± 0.08	70.6	3 ± 3
				33.0 ± 0.1	0.49 ± 0.01					
1.5	40	129	0.23			17.0 ± 0.4	3.5 ± 0.1	0.50 ± 0.03	76.3	14 ± 3
		142	0.18	34.7 ± 0.01	0.48 ± 0.03					
7.4	25					19.3 ± 0.5	1.1 ± 0.5	0.20 ± 0.01	66.4	7.3 ± 0.5
7.4	40					13 ± 1	5.1 ± 0.2	0.44 ± 0.03	60.9	7.6 ± 0.5

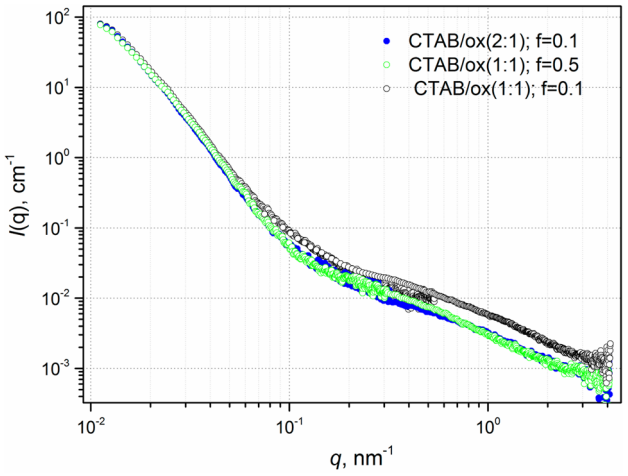

Figure 10. SAXS curves for solutions of ox(1:1), and ox(1:2) polymers and CTAB taken at T = 25 °C.

fraction for the iPrOx group in the different polymers allows for an assessment of the influence of the rest groups in the polymer on the thermosensitivity of iPrOx (Figure 3c). Considering our previous conclusion about the statistical arrangement of the BuOx and iPrOx groups in the central block of polymers and the independent character of the MeOx moieties, it makes sense to consider the influence of just the BuOx groups on the thermosensitivity of iPrOx. Here, we do not exclude the influence of the MeOx groups at all; instead, we attribute this influence solely to the shift in the position of CPT. The curve for iPrOx in the 2c-triblock copolymer reflects this situation (Figure 3c). Moreover, we detect a sharp transition in the separation fraction for the 2c-triblock copolymer as well. The addition of BuOx groups decreases the slope of the curve, and this change does not correlate with the BuOx group content in the polymer. We must thus consider some general factors related to the complex structure of the polymer molecules. While the thermosensitive groups promote a thermosensitive response of the hydrophobic groups and exert fewer effects on the hydrophilic groups, and the hydrophilic groups shift the transition temperature of the whole molecule, the hydrophobic groups could exert their effect by influencing the formation of hydrophobic microdomains. Consequently, the difference in the number of iPrOx and BuOx groups would define the hydrophobicity of the central block. A smaller difference would lead to a less thermoresponsive and more hydrophobic central block. The previous results confirm our assumption[7] (Supporting Information Table 1S). Thus, the slope of the curve in Figure 3 would reflect the hydrophobicity of the central entity. A smaller slope of the curve corresponds to a more hydrophobic central block.

The observed temperature behavior of the different blocks leads to new questions. Namely, will the difference in the nature of the blocks affect their interaction with amphiphilic molecules? To answer this question, we performed ITC experiments where pure polymer solutions were titrated by solutions of ionic surfactants (SDS or CTAB). These surfactants were chosen based on the different binding strengths that were recently reported for PNIPAM and PEO nonionic polymers.[23−26]

Three different temperatures were chosen for ITC analysis: 15, 25, and 41 °C; these temperatures correspond to the single molecule, large aggregate (or loose nanoparticle), and compact nanoparticle states of the polymer, respectively. The experiment was performed by sequentially adding the surfactant (SDS or CTAB) to the polymer solution. The previous data indicate that we can consider our 3c-triblock copolymers to be similar to Pluronic molecules with central thermosensitive/hydrophobic blocks and terminal hydrophilic blocks. This assumption allows us to use the system of Pluronic molecules with surfactants as a basis for further analysis of our systems.

Some experiments were conducted using thermoresponsive systems of PEO−PPO−PEO block copolymers with different

Table 4. Fitting Parameters for ox(1:1), ox (1:2), and SDS at T = 25 °C

copolymers	f	R, Å	sigma	R_g, Å	RHS, Å	f_b, 10^{-2}
ox(1−1)	7.4	19.3 ± 0.2	0.29 ± 0.01	1.7 ± 0.3	66.4 ± 0.1	7.0 ± 0.3
ox(1−2)	5.0	17.2 ± 0.9	0.47 ± 0.03	3.5 ± 0.3	78.8 ± 0.1	7.6 ± 0.3

dx.doi.org/10.1021/jp5011296 | J. Phys. Chem. B 2014, 118, 4940−4950

length of blocks in combination with SDS and CTAB.[11−13] We begin our consideration of the interaction between an ionic surfactant and nonionic 3c-triblock copolymer with the case of the anionic SDS. Analysis of the interaction of the F127 Pluronic molecule with SDS shows that the process can be described in a few stages. The number of stages depends on whether the polymer is in a state above or below the CPT. At temperatures below CPT, the polymer is in a dissolved state where single molecules can be detected. In this case, the ITC measurements are characterized by a single peak and two processes: an initial endothermic process followed by an exothermic process that finally proceeds to the formation of unimodal micelles of the surfactant.[11] This type of ITC curve is characteristic of a nonionic polymer and ionic surfactant. We observed similar behavior for our polymers at 15 °C (Figure 4a,b). Three important parameters could be determined from the ITC data: cac (critical aggregation concentration) = the concentration of the onset of the interaction between a polymer and surfactant, C_2 = the concentration at which micelles of the surfactant begin to form, and ΔH = the enthalpy of interaction. The data at 15 °C show a difference in the enthalpy of interaction: 3.6 kcal/mol for ox(1:2) and 10.4 kcal/mol for ox(2:1) (Figure 4a,b). Because we measured the transfer of the polymer from a bad solvent (water) to a good solvent (surfactant solution), one can conclude that this process should be more preferable for a more hydrophobic polymer, such as ox(2:1). The ox(1:2) at 15 °C was far from the CPT and did not show significant aggregation behavior.

As the temperature increases up to 25 °C, the polymers change their conformation from a single molecule to a large aggregate or a loose nanoparticle. In this situation, we can observe four processes in the ITC curve (Figure 4a,b): an initial endothermic process (1) followed by a strong exothermic process (2) with a subsequent strong endothermic process (3) and finally a weak exothermic process with merging of the measured curve to the curve for a pure surfactant (4). Similar behavior was observed in the interaction of F127 and other Pluronic molecules with SDS above CPT.[11,13,27] A very well-composed and reasoned explanation for such behavior was proposed by Li and Xu et al. The authors suggested that the first stage includes binding of the surfactant to the polymer aggregates and the formation of stable complexes. In the second stage, the sequential addition of SDS promotes the breakdown of the complexes to smaller mixed aggregates. This process continues until all aggregated structures are dissociated. The second stage may also include some interaction between the dissociated molecules of the polymer and the surfactant, but that process plays a leading role in the third stage. The last stage is the release of some bonding water from the polymer−surfactant hybrid micelles, followed by the formation of pure micelles of the surfactant (Figure 4b). Increases in the temperature up to 41 °C, where the polymer molecules are in a compact nanoparticle state, do not influence the form of the curve; the increases only make the exothermic process more explicit. In fact, the dimension of the exothermic peak is a function of particles compactness. The polymer ox(2:1) at 41 °C has more compact structure (ca. 25 nm) than the polymer ox(1:2) (ca. 1000 nm) and displays a more pronounced exothermic peak on the enthalpogram. It is worth to mention that we did not observe any significant changes in the values of cac and C_2 for ox(1:2) and ox(2:1) at 15 and 25 °C or at 41 °C. For our polymers, cac was almost constant in the range of 0.15−0.35 mM for any triblock copolymers and at any measured temperature (Figure 4a,b and Figure 2S). This result indicates that neither the hydrophobicity (hydrophilicity) nor the conformation of the polymer affects the strength of the interaction between SDS and the polymer. Moreover, the corresponding value of cac for F127 with SDS was found to be 0.35 mM. Because cmc = 8.4 mM for the pure SDS solution, one can conclude that the interaction of the SDS surfactant with the amphiphilic block copolymers is strong and non-specific (Table 2). Furthermore, we also detected the binding of SDS to the hydrophilic MeOx, which also supports our assumption about the nonspecific nature of the interaction of the SDS surfactant (Figure 3S).

The same analysis logic can be applied to the system of polymers with the cationic surfactant CTAB (Figure 5 and Figure 4S). We have observed the typical character of the curve for all polymers in the presence of CTAB.[13,27] However, there are some new and notable findings. The concentration dependence of the enthalpy changes shifted to a higher surfactant concentration than that for the case of the SDS experiment. Moreover, we did not detect any significant exothermic effect in the thermograms. Both of these factors could be explained by a weaker interaction with the compounds. Although ionic surfactants act in a similar manner, the differences in the size and charge of the headgroup may affect the strength of the interaction between the polymer and the surfactant. The parameter cac, which describes the onset of the binding process, is usually used to characterize the interaction strength. It is well-known that the cationic surfactant CTAB has a sterically more demanding ionic group (quaternary ammonium) at the end of the molecule compared with the ionic one (sulfate) in the anionic SDS.[12,13] This difference may explain why the interaction between the polymer and CTAB only starts at a cac = 0.7 mM surfactant concentration (cmc = 1.2 mM). In contrast, SDS did not show significant steric repulsions and the interaction began at a concentration of 0.35 mM (cmc = 8.4 mM). Another feature of the CTAB−polymer interactions is the existence of two different critical aggregation concentrations depending on the state of the polymer system. As mentioned above, the cac for the molecular conformation of a polymer was found to be 0.7 mM CTAB, while cac = 0.07 mM was detected for the polymer aggregates. This results reveals the complex but highly specific binding of CTAB to the macromolecule (Table 2).

To test the previously suggested mechanism for the interactions of the polymers with ionic surfactant, SAXS experiments were conducted. In these experiments, we tried to trace the evolution of the complexes as the composition ratio (f = C(surf.)/C(pol)) increased and to assess the temperature dependence of the process. For this reason, the f values for the experiment were selected in accordance with the characteristic processes on the ITC thermograms (Figure 4 and Figure 2S): 0.5 (C(sds) = 0.7 mM), 1.0 (1.4 mM), 1.5 (2.1 mM), and 7.4 (10.4 mM). The scattering curves for T = 25 °C show some changes with increasing composition ratio f (Figure 6a). At low q values, an upturn is visible for f = 0 and 0.5. At high q values, the scattering curve is a smooth function of q. With increasing SDS concentration, the upturn at low q values decreases, whereas at high q values, a side peak becomes clearly resolved. Similar behavior was observed at T = 40 °C (Figure 6b). The only difference between two temperatures is that the upturn is much more pronounced at T = 40 °C.

The interpretation of the scattering curves presented in Figure 6a,b is rather straightforward. The upturn at low values

dx.doi.org/10.1021/jp5011296 | J. Phys. Chem. B 2014, 118, 4940−4950

of q obviously results from the presence of large particles in the solution. The disappearance of the upturn should be related to particle decomposition. Moreover, the depression in the scattering intensity as $q \rightarrow 0$ at $f = 7.4$ and the appearance of a peak at $q = 0.4$ nm^{-1} for both temperatures are manifestations of the structure factor caused by the repulsion of the SDS micelles (Figure 7).

Previously, several SANS and SAXS experiments on the interaction of SDS with neutral polymers were reported.[28−35] In the classical work of Cabanne and Duplessix,[31] a contrast variation study was utilized to obtain structural information about PEO−SDS complexes. It was established that single PEO chains enhance the micellization of SDS molecules. Moreover, the structure of these complexes could be characterized by the hard-sphere model with SDS micelles of 2 nm with a separation distance of 9 nm between micelles. The presence of charged SDS micelles disrupts the conformation of PEO chains, making them more expanded and forming a pearl-necklace structure.

A similar conclusion was obtained for the PEO−SDS system by Suss et al. on the basis of cryo-TEM and SAXS experiments.[32] A hollow sphere model was used as a fitting function. The calculated radius was found to be 2.1 nm for SDS micelles in a mixture of 2 wt % SDS and 1% PEO and 2.5 nm for the pure 2.0% aqueous solution of SDS. A radius of 2.3−2.5 nm for the free SDS micelles was reported by Itri and Amral.[33,36] Similar results were also observed for the PVP−SDS system.[34]

To fit the scattering curves, several models could be utilized. In our work, we selected two models as the most appropriate ones: the model of a generalized Gaussian coil and the model of a sphere with an attached Gaussian coil. The generalized Gaussian coil model (parameters: R_g = radius of gyration of a polymer chain; ν = Flory exponent) was taken for the case of $f = 0$ and 0.5, whereas for $f > 0.5$, the sphere with an attached Gaussian coil model seems more plausible. This model was utilized instead of the hard sphere or hollow sphere model that previous authors utilized to analyze polymer−SDS aggregates.[32,33] As shown in Figure 7, the hard sphere fitting functions correctly describe the structure peak but vanish rapidly at $q > 1$ nm^{-1}, thus failing to describe the second peak. Because the scattering from the buffer was properly subtracted, there is a contribution to the scattered intensity apart from the hard sphere that should be taken into account. It is logical to assume that some pMeOx chains might be present on the surface of the SDS micelles. Therefore, the model of the sphere with an attached Gaussian coil was tested (parameters: R = radius of the core; R_g = radius of gyration of the outer shell; sigma = polydispersity). In some cases where an upturn at low q values was visible ($T = 40$ °C), we added a second contribution, the hard sphere model (R_{big} = radius of hard sphere; sigma = polydispersity) with Schultz−Zimm polydispersity. To account for the repulsive interactions, the classical Percus−Yevik structure factor was applied (parameters: RHS = hard sphere repulsion radius; f_b = volume fraction of hard spheres). The resulting fitting functions are presented in Figure 6.

Together with the Percus−Yevik structure factor, the fractal $\exp(-\alpha)$ structure factor described in ref35 was tried. That structure factor was not able to correctly describe the correlation peak of the curve. Thus, we can conclude that the pearl-necklace model is not applicable in our case due to the shorter contour length of polyoxazolines.

The fitting of the SAXS data also supports the conclusions drawn from the ITC experiments. The "structure-sequence" plot summarizes the obtained regularities for different concentrations of surfactants (Figure 9). At $f = 0.5$, which corresponds to the first exothermic process at 0.7 mM SDS (Figure 9, pink line, pink plot), the coexistence of the polymer in a coil conformation with 20.0 nm particles is visible in the SAXS data (Figure 7a and Table 3). The chain conformation of the copolymer at $f = 0.5$ is almost identical to the one in a surfactant-free solution ($f = 0$, Table 3) (Figure 9, blue line, blue plot). Moreover, the size and excluded volume exponent indicate that the ox(1:1) copolymer is in the swollen Gaussian chain conformation. The increase in the f value changes the SAXS pattern. At $f = 1$ (C(sds) = 1.4 mM) (Figure 9, green line, green plot), no large particles are observable on the SAXS curves at low q values at $T = 25$ °C (Figure 6a). Obviously, the large aggregates visible at $f = 0.5$ were disrupted with the higher SDS content, thus confirming the hypothesis drawn from the ITC data in which process 2 (Figure 9, pink line) is a breaking down of large mixed aggregates. Moreover, a small depression in the scattered intensity is witnessed at low q values (0.1−0.3 nm^{-1}), and a tiny upturn starts to grow at high q values ($q > 1$ nm^{-1}). This upturn is obscured by noise and is considered a deviation from Gaussian behavior. That fact impels us to find a more appropriative model to describe the visible features. The model of a sphere with an attached Gaussian coil seems more promising and seems to reflect the actual situation, as mentioned above. We also admit that the generalized Gaussian coil model is still applicable in this case (Table 2). A similar situation was observed for $f = 1.5$ as well. The only difference between the curves is a better manifestation of the peak at $q > 1$ nm^{-1}. All of these findings confirm our previous assumption from the ITC data about the manner of the interaction between the polymer and surfactant. Thus, one can propose that the disruption of the large aggregates and the formation of nonstoichiometric complexes between SDS and the copolymer occur in the second and third stages of the reaction (Figure 9, pink and green line, respectively).

The situation is not very different at $T = 40$ °C (Figure 6b and Table 3). Large particles coexist in the solution together with the single copolymer chains. However, in contrast with the situation at 25 °C, the large particles remain up to $f = 7.4$. The increase in the hydrophobicity of the copolymer due to the thermoresponsive nature of the iPrOx blocks plays a critical role here. The number of hydrophobic blocks increases to increase the number of large aggregates in the solution. The addition of 1.4 mM SDS ($f = 1.0$) is simply insufficient to break down all aggregates at this temperature.

The interpretation of the SAXS curves at $f = 7.4$ is straightforward (Figure 9, red line, red plot). The second peak is well resolved and indicates that hybrid micelles are formed in the solution. The core of such micelles is composed of SDS molecules bound to a copolymer chain. Moreover, no large particles are visible on the SAXS curves at either temperature. One can conclude that an ample amount of SDS was added to the solution, thus successfully preventing polymer aggregation. In contrast with the situation for high molecular weight homopolymers, such as PEO or PNIPAM, no pearl-necklace structure is formed for the copolymer ox(1:1), most likely due to the short length of the involved polymer chains. We have found that the size of the hybrid micelles 1.8−2.0 nm was in good agreement with the previously reported data for SDS−nonionic polymer complexes and less than the

dx.doi.org/10.1021/jp5011296 | J. Phys. Chem. B 2014, 118, 4940−4950

dimensions of pure SDS micelles in the polymer free solution. Interestingly, the dimension of the micellar core at 40 °C is less than that at 25 °C, while the radius of gyration of the Gaussian chains in the micellar shell and the polydispersity are higher. That fact can be explained again by the polymer thermosensitivity. As the polymer becomes more hydrophobic with increasing temperature, the tendency to move from the bad solvent (water) to the good one (surfactant micelles) increases. Finally, when the rearrangement is completed, the hydrophobic groups together with the surfactant molecules form a compact core, while the hydrophilic groups of the polymer extend to the water. The value f = 7.4 (10.4 mM of SDS) corresponds to process 4 (Figure 9, red line). It is the last process which brings about the interaction between the polymer and surfactant. Above that point, only pure micelles of the surfactant are observed to form.

The SAXS experiment shows that hybrid micelles could be formed for all copolymers regardless of their initial structure (Figure 8 and Table 4). The structure of such micelles is only determined by the amount of SDS in solution. In contrast, CTAB interacts much more weakly with the copolymer, as can be shown in the SAXS data (Figure 9). Large aggregates are observed on the SAXS curves even at high values of f.

CONCLUSIONS

We have investigated the temperature-dependent solution behavior of nonionic amphiphilic polymers with a complex nature. Triblock copolymers MeOx−(co-iPrOx-BuOx)−MeOx show thermoresponsive properties. As the temperature increase, the polymers transform from single molecules to loose aggregates to compact nanoparticles. We demonstrated that the ratio iPrOx/MeOx is a critical for the value of CPT, while the difference in BuOx-iPrOx can be attributed to the hydrophobicity of the central block of the polymers. Greater hydrophobicity in the central block of the polymer corresponded to the formation of looser aggregates at high temperature. The addition of ionic surfactant leads to a rearrangement of the polymer molecules and finally to the formation of complexes between the polymer and surfactant. The interaction process is described in detail along with the structure of the formed complexes. Analysis of the interaction shows a strong and nonspecific reaction with the anionic surfactant SDS, but the binding of cationic CTAB is weak but highly sensitive to the polymer state. Nevertheless, we can refer the structure of our polymers to the structure of the Pluronic molecule PEO−PPO−PEO despite the statistical arrangement of the hydrophobic (BuOx) and thermoresponsive (iPrOx) groups in the central part. These findings play a critical role in understanding the behavior of poly(2-alkyl-2-oxazoline)-based micellar drug delivery systems, where the solution behavior is driven by polymer−polymer, polymer−drug, and drug−drug interactions.

ASSOCIATED CONTENT

Supporting Information

DLS data for BlockOx; table of physicochemical characteristics of the block polyoxazolines; ITC data for ox(1:1) and SDS; ITC data for MeOx, SDS, and CTAB; ITC data for ox(1:1), ox(2:1), and CTAB. This material is available free of charge via the Internet at http://pubs.acs.org.

AUTHOR INFORMATION

Corresponding Author

*Tel + 420 296 809 291, Fax +420 296 809 410, e-mail filippov@imc.cas.cz (S.F.).

Notes

The authors declare no competing financial interest.

ACKNOWLEDGMENTS

We gratefully acknowledge the European Synchrotron Radiation Facility (Grenoble, France) for providing synchrotron beam time (SC3113) and the Grant Agency of the Czech Republic, Project P205/11/1657. The authors thank the Academy of Sciences of the Czech Republic, Grant No. M200501201; the Ministry of Industry and Trade, Grant MPO TIP No. FR-TI4/625 financial support No. CZ09-DE06/2013-2014 from the ASCR−DAAD Programme PPP 2013-2014 and the EU FP7 program, I3 access Grant BioStruct-X, project Number 283570.

REFERENCES

(1) Hoogenboom, R. Poly(2-oxazoline)s: A Polymer Class with Numerous Potentia Application. *Angew. Chem.* **2009**, *48*, 7978−7994.
(2) Sedlacek, O.; Monnery, B. D.; Filippov, S. K.; Hruby, M.; Hoogenboom, R. Poly(2-Oxazoline)s − Are They More Advantageous for Biomedical Applications Than Other Polymers? *Macromol. Rapid Commun.* **2012**, *33*, 1648−1662.
(3) Viegas, T. X.; Bentley, M. D.; Harris, J. M.; Z, F.; Yoon, K.; Dizman, B.; Weimer, R.; Mero, A.; Pasut, G.; Veronese, F. M. Polyoxazoline: Chemistry, Properties, and Applications in Drug Delivery. *Bioconjugate Chem.* **2011**, *22*, 976−986.
(4) Luxenhofer, R.; Han, Y.; Schulz, A.; Tong, J.; He, Z.; Kabanov, A. B.; Jordan, R. Poly(2-oxazoline)s as Polymer Therapeutics. *Macromol. Rapid Commun.* **2012**, *33*, 1613−1631.
(5) Zhang, N.; Luxenhofer, R.; Jordan, R. Thermo-Responsive Poly(2-oxazoline) Molecular Brushes by Living Ionic Polymerization: Kinetic Investigations of Pendant Chain Grafting and Cloud Point Modulation by Backbone and Side Chain Length Variation. *Macromol. Rapid Commun.* **2012**, *213*, 973−981.
(6) Zschoche, S.; Rueda, J.; Boyko, V.; Krahl, F.; Arndt, K.-F.; Voit, B. Thermo-Responsive Nanogels Based on Poly[NIPAAm-graft-(2-alkyl-2-oxazoline)]s Crosslinked in the Micellar State. *Macromol. Chem. Phys.* **2010**, *211*, 1035−1042.
(7) Hruby, M.; Filippov, S. K.; Panek, J.; Novakova, M.; Mackova, H.; Kucka, J.; Vetvicka, D.; Ulbrich, K. Polyoxazoline Thermoresponsive Micelles as Radionuclide Delivery Systems. *Macromol. Biosci.* **2010**, *10*, 916−924.
(8) Yu, G.; Deng, Y.; Dalton, S.; Wang, Q.; Attwood, D.; Price, C.; Booth, C. Micellisation and Gelation of Triblock Copoly(oxyethylene/oxypropylene/oxyethylene), F127. *J. Chem. Soc., Faraday Trans.* **1992**, *88*, 2537−2544.
(9) Wanka, G.; Hoffmann, H.; Ulbricht, W. The Aggregation Behavior of Poly-(oxyethylene)-poly-(oxypropylene)-poly-(oxyethylene)-Block-Copolymers in Aqueous Solution. *Colloid Polym. Sci.* **1990**, *268*, 101−117.
(10) Escobar-Chavez, J. J.; Lopez-Cervantes, M.; Naik, A.; Kalia, Y. N.; Quintanar-Guerrero, D.; Ganem-Quintanar, A. Applications of Thermoreversible Plyronic F-127 Gels in Pharmaceutical Formulations. *J. Pharm. Pharm. Sci.* **2006**, *9*, 339−358.
(11) Li, Y.; Xu, R.; Bloor, D. M.; Holzwarth, J. F.; Wyn-Jones, E. The Binding of Sodium Dodecyl Sulfate to the ABA Block Copolymer Pluronic F127 ($EO_{97}PO_{69}EO_{97}$)-Electromotive Force, Microcalorimetry and Light Scattering Studies. *Langmuir* **2000**, *16*, 10515−10520.
(12) Li, Y.; Xu, R.; Couderc, S.; Bloor, D. M.; Holzwarth, J. F.; Wyn-Jones, E. Binding of Tetradecyltrimethylammonium Bromide to the ABA Block Copolymer Pluronic F127 (EO97 PO69 EO97):

Electromotive Force, Microcalorimetry, and Light Scattering Studies. *Langmuir* **2001**, *17*, 5742−5747.
(13) Li, Y.; Xu, R.; Couderc, S.; Bloor, D. M.; Wyn-Jones, E.; Holzwarth, J. F. Binding of Sodium Dodecyl Sulfate (SDS) to the ABA Block Copolymer Pluronic F127 (EO97PO69EO97): F127 Aggregation Induced by SDS. *Langmuir* **2001**, *17*, 183−188.
(14) Hecht, E.; Hoffmann, H. Interaction of ABA Block Copolymers with Ionic Surfactants in Aqueous Solution. *Langmuir* **1994**, *10*, 86−91.
(15) Hecht, E.; Mortensen, K.; Gradzielski, M.; Hoffmann, H. Interaction of ABA Block Copolymers with Ionic Surfactants: Influence on Micellization and Gelation. *J. Phys. Chem.* **1995**, *99*, 4866−4874.
(16) Konarev, P.; Volkov, V.; Sokolova, A.; Koch, M.; Svergun, D. PRIMUS: a Windows PC-Based System for Small-Angle Scattering Data Analysis. *J. Appl. Crystallogr.* **2003**, *36*, 1277−1282.
(17) Konarev, P. V.; Petoukhov, M. V.; Volkov, V. V.; Svergun, D. I. ATSAS 2.1, a Program Package for Small-Angle Scattering Data Analysis. *J. Appl. Crystallogr.* **2006**, *39*, 277−286.
(18) Spevacek, J.; Dybal, J.; Starovoytova, L.; Zhigunov, A.; Sedlakova, Z. Temperature-induced Phase Separation and Hydration in Poly(N-vinylcaprolactam) Aqueous Solutions: a Study by NMR and IR Spectroscopy, SAXS, and Quantum-chemical Calculations. *Soft Matter* **2012**, *8*, 6110−6119.
(19) Aseyev, V. O.; Tenhu, H.; Winnik, F. M. Temperature Dependence of the Colloidal Stability of Neutral Amphiphilic Polymers in Water. *Adv. Polym. Sci.* **2006**, *196*, 1−85.
(20) Guillermo, A.; Addad, J. P.; Bazile, J. P.; Duracher, D.; Elaissari, A.; Pichot, C. NMR Investigations into Heterogeneous Structures of Thermosensitive Microgel Particles. *J. Polym. Sci., Part B* **2000**, *38*, 889−898.
(21) Hofmann, C.; Schonhoff, M. Dynamics and Distribution of Aromatic Model Drugs in the Phase Transition of Thermoreversible Poly(N-isopropylacrylamide) in Solution. *Colloid Polym. Sci.* **2012**, *290*, 689−698.
(22) Kriz, J.; Dybal, J. Cooperative Preassociation Stages of PEO−PPO−PEO Triblock Copolymers: NMR and Theoretical Study. *J. Phys. Chem. B* **2010**, *114*, 3140−3151.
(23) Loh, W.; Teixeira, L. A. C.; Lee, L. T. Isothermal Calorimetric Investigation of the Interaction of Poly(N-isopropylacrylamide) and Ionic Surfactants. *J. Phys. Chem. B* **2004**, *108*, 3196−3201.
(24) Abuin, E.; Leon, A.; Lissi, E.; Varas, J. M. *Colloids Surf., A* **1999**, *147*, 55−65.
(25) Nambam, J. S.; Philip, J. Effects of Interaction of Ionic and Nonionic Surfactants on Self-Assembly of PEO−PPO−PEO Triblock Copolymer in Aqueous Solution. *J. Phys. Chem. B* **2012**, *116*, 1499−1507.
(26) Niemiec, A.; Loh, W. Interaction of Ethylene Oxide−Propylene Oxide Copolymers with Ionic Surfactants Studied by Calorimetry: Random versus Block Copolymers. *J. Phys. Chem. B* **2008**, *112*, 727−733.
(27) Cardoso da Silva, R.; Olofsson, G.; Schillen, K.; Loh, W. Influence of Ionic Surfactants on the Aggregation of Poly(Ethylene Oxide)−Poly(Propylene Oxide)−Poly(Ethylene Oxide) Block Copolymers Studied by Differential Scanning and Isothermal Titration Calorimetry. *J. Phys. Chem. B* **2002**, *106*, 1239−1246.
(28) Almgren, M.; Brown, W.; Hvidt, S. Self-Aggregation and Phase Behavior of Poly(ethylene oxide)-poly(propylent oxide)-poly(ethylene oxide) Block Copolymer in Aqueous Solution. *Colloid Polym. Sci.* **1995**, *273*, 2−15.
(29) Almgren, M.; Garamus, V. M.; Asakawa, T.; Nan, J. Contrast Variation SANS Investigation of Composition Distributions in Mixed Surfactant Micelles. *J. Phys. Chem. B* **2007**, *111*, 7133−7141.
(30) Garamus, V. M. Formation of Mixed Micelles in Salt-Free Aqueous Solutions of Sodium Dodecyl Sulfate and $C_{12}E_6$. *Langmuir* **2003**, *19*, 7214−7218.
(31) Cabane, B.; Duplessix, R. Organization of Surfactant Micelles Adsorbed on a Polymer Molecule in Water: a Neutron Scattering Study. *J. Phys. (Paris)* **1982**, *43*, 1529−1542.
(32) Süss, D. C.; Cohen, Y.; Talmon, Y. The Microstructure of the Poly(ethylene oxide)/Sodium Dodecyl Sulfate System Studied by Cryogenic-Temperature Transmission Electron Microscopy and Small-Angle X-ray Scattering. *Polymer* **1995**, *36*, 1809−1815.
(33) Itri, R.; Amaral, L. C. Distance Distribution Function of Sodium Dodecyl Sulfate Micelles by X-ray Scattering. *J. Chem. Phys.* **1991**, *95*, 423−427.
(34) Cattoz, B.; de Vos, W. M.; Cosgrove, T.; Crossman, M.; Prescott, S. W. Manipulating Interfacial Polymer Structures through Mixed Surfactant Adsorption and Complexation. *Langmuir* **2012**, *28*, 6282−6290.
(35) Santos, S. F.; Zanette, D.; Fischer, H.; Itri, R. A Systematic Study of Bovine Serum Albumin (BSA) and Sodium Dodecyl Sulfate (SDS) Interactions by Surface Tension and Small Angle X-ray Scattering. *J. Colloid Interface Sci.* **2003**, *262*, 400−408.
(36) Almgren, M.; Gimel, J. C.; Wang, K.; Karlsson, G.; Edwards, K.; Brown, W.; Mortensen, K. SDS Micelles at High Ionic Strength. A Light Scattering, Neutron Scattering, Fluorescence Quenching, and CryoTEM Investigation. *J. Colloid Interface Sci.* **1998**, *202*, 222−231.